International Journal of Women's Health

Dovepress
Taylor & Francis Group

Open Access Full Text Article

ORIGINAL RESEARCH

CXCL8 Promotes the Progression of Vulvar Squamous Cell Carcinoma and Serves as a Potential Prognostic Biomarker

Xing-Yan Wu[1,2,*], Yong-Jun Zhang[1,*], Jing-Man Li[1,*], Shi-Yi He[1], Xiao-Juan Yang[1], Jie-Mei Wang[3], Yue Jia[1], Yi-Han Lu[4], Hong-Ping Zhang[1]

[1]Department of Gynecology, The Third Affiliated Hospital of Kunming Medical University, Yunnan Cancer Hospital, Peking University Cancer Hospital Yunnan, Kunming, Yunnan, People's Republic of China; [2]Department of Gynecology, Zhaotong First People's Hospital, Zhaoyang, Yunnan, People's Republic of China; [3]Department of Obstetrics and Gynecology, Kunming Third People's Hospital, Kunming, Yunnan, People's Republic of China; [4]Department of Oncology, The Second People's Hospital of Kunming, Kunming, Yunnan, People's Republic of China

*These authors contributed equally to this work

Correspondence: Hong-Ping Zhang, Department of Gynecology, The Third Affiliated Hospital of Kunming Medical University, Yunnan Cancer Hospital, Peking University Cancer Hospital Yunnan, Kunming, Yunnan, People's Republic of China, Email kmzhp@126.com; Yi-Han Lu, Department of Oncology, The second People's hospital of kunming, Kunming, Yunnan, People's Republic of China, Email 13888506336@139.com

Background: Vulvar squamous cell carcinoma (VSCC), although rare, poses substantial clinical challenges due to frequent late-stage diagnosis, quality-of-life-impairing surgical interventions, and the availability of limited therapeutic options following recurrence. Therefore, exploration of the pathogenesis of vulvar cancer, and identification of effective therapeutic targets based on the biological pathways of disease progression, offer great value in improving patients' survival duration and quality of life.

Patients and Methods: Herein, we investigated the influence of C-X-C motif chemokine ligand 8 (CXCL8) on the proliferation of vulvar squamous cancer cells and the underlying mechanisms, as well as their influence on the prognosis of patients with VSCC.

Results: Using a combination of RNA sequencing and Gene Expression Omnibus (GEO) database analysis, CXCL8 was identified as a differentially expressed gene in vulvar cancer tissue in comparison with adjacent normal tissue. Immunohistochemical analysis of selected clinical specimens revealed that CXCL8 was statistically upregulated in vulvar squamous cancer tissues in comparison with adjacent normal tissue, and this upregulation was correlated with shorter progression-free survival and overall survival. Functional assays demonstrated that CXCL8- mediated proliferation enhancement in VSCC cell lines (SW962/A431) in a dose- and time-dependent manner. Cell cycle analysis showed that exogenous CXCL8 drove a G0/G1-to-G2/M phase transition in SW962 and A431 cells. Transcriptomic profiling explored CXCL8-activated pathways, including cytokine-cytokine receptor interaction, transforming growth factor (TGF)-β signaling pathway, and tryptophan metabolism.

Conclusion: These findings highlight CXCL8 as a potential prognostic biomarker for VSCC and underscore its role in driving tumor proliferation, providing a rationale for targeting CXCL8 in vulvar cancer therapy.

Keywords: vulvar squamous cell carcinoma, CXCL8, proliferation, progression-free survival, overall survival

Introduction

Vulvar cancer is a rare gynecologic malignancy, accounting for approximately 5% of all female reproductive system tumors.[1] The incidence and mortality rates associated with vulvar cancer have increased recently, and this increase has been accompanied by a noticeable trend toward younger age at diagnosis.[2] Epidemiological data from the United States in 2025 shows that vulvar cancer accounts for approximately 7480 new cases annually, with an associated mortality of 1,770 deaths.[3] A major concern is that many patients fail to receive timely treatment, exacerbating challenges in screening, diagnosis, and therapeutic interventions. This issue is particularly obvious in Yunnan province, where socioeconomic disparities, including a high concentration of ethnic minorities, economic underdevelopment, low education levels, and

https://doi.org/10.2147/IJWH.S569683
Received: 23 September 2025
Accepted: 24 February 2026
Published: 16 March 2026

deeply ingrained traditional beliefs, contribute to delays in seeking medical consultation. Due to the complex anatomical location of vulvar cancer, its surgical treatment frequently requires multidisciplinary collaboration, incorporating expertise from orthopedic, urologic, and colorectal surgical teams.[4] However, this approach imposes substantial demands on medical resources and profoundly affects patients' postoperative quality of life. Consequently, investigating and developing effective treatment strategies to reduce morbidity and enhance these patients' quality of life are of great importance.

In contemporary clinical practice, therapeutic strategies for vulvar cancer are stratified according to tumor stage. Early-stage disease is conventionally treated with radical vulvectomy accompanied by regional lymph node dissection.[5] However, in cases involving advanced-stage disease, disease recurrence, or metastasis, clinicians frequently encounter extensive lesion involvement, and surgical intervention may cause substantial iatrogenic damage to adjacent tissues, including the anus and rectum.[6] Postoperative vulvar reconstruction is also challenging, and often result in suboptimal functional restoration and diminished quality of life.[7] Despite these limitations, surgical resection is the primary intervention for such cases, given the paucity of effective alternatives. Furthermore, vulvar cancer often demonstrates poor responsiveness to chemotherapy, whereas radiotherapy frequently causes localized vulvar skin ulceration due to the poor tolerance of vulvar skin and mucous membrane.[8,9] Consequently, neither surgical nor conventional adjuvant modalities have substantially improved survival outcomes or restored functional status for this patient population.[10] These clinical limitations underscore the urgent need for translational research to elucidate the molecular pathogenesis of vulvar cancer and develop new therapeutic targets.

C-X-C motif chemokine ligand 8 (CXCL8), also known as interleukin (IL)-8, is a core member of the C-X-C chemokine family and play a critical role in the development, metastasis, and angiogenesis of multiple types of solid tumors.[11,12] Mechanistically, CXCL8 promotes tumor proliferation and survival by activating key intracellular signaling pathways, including the phosphoinositide 3-kinase (PI3K)/protein kinase B (AKT) and mitogen-activated protein kinase (MAPK) pathways.[13,14] Furthermore, it is a potent inducer of epithelial-mesenchymal transition (EMT), which enhances the migration and invasiveness abilities of vulvar cancer cells.[15] Clinicopathological analyses have shown that the expression level of CXCL8 is positively correlated with tumor blood vessel density in diverse solid tumors, positioning CXCL8 inhibition as a promising anti-angiogenic strategy for impeding tumor progression.[16] Beyond its pathophysiological roles, CXCL8 has emerged as both a valuable diagnostic biomarker and a compelling therapeutic target. Previous studies have documented marked elevations of CXCL8 levels in both serum and tissue samples from cancer patients, implicating its diagnostic utility.[17] Importantly, high CXCL8 expression has been shown to be robustly associated with poor prognostic indicators, including advanced tumor stage, high recurrence rates, and diminished survival, establishing its prognostic significance.[18,19] However, the functional roles and therapeutic potential of CXCL8 in vulvar cancer remain largely unexplored.

The present study systematically investigated the functional role of CXCL8 in promoting vulvar cancer cell proliferation in vitro and tumor growth in an established xenograft vulval cancer model in vivo. Clinical databases were integrated to evaluate the utility of CXCL8 as a diagnostic and prognostic biomarker, with the aim of identifying novel molecular targets and providing theoretical support for precision medicine in vulvar cancer. These findings may provide new approaches for the treatment of vulvar cancer.

Materials and Methods

Patient Enrollment and Clinical Sample Collection

In this retrospective study, we enrolled 60 consecutive patients with histologically confirmed vulvar squamous cell carcinoma (VSCC) who underwent primary surgical resection at Yunnan Cancer Hospital (the Third Affiliated Hospital of Kunming Medical University) between January 2015 and January 2019. The inclusion criteria were defined as follows: (1) primary curative-intent surgical treatment; (2) postoperative histopathological confirmation of VSCC; (3) complete available preoperative-tumor marker, and imaging data, and postoperative pathological data; and (4) complete available follow-up documentation. Exclusion criteria were as follows: (1) incomplete clinical documentation or unavailable postoperative tissue specimens; (2) history of or concurrent other malignancies; (3) non-standardized treatment at our institution; and (4) presence of acute infectious diseases, contagious illnesses, severe liver/kidney dysfunction, or severe uncontrollable systemic diseases.

Clinical specimens were collected within 30 min after surgical resection. All tumor tissues underwent pathological verification through hematoxylin-eosin (HE) staining and immunohistochemical analysis at the Pathology Department at the Third Affiliated Hospital of Kunming Medical University. This use of paraffin-embedded tissue samples received ethical approval from the Committee of the Third Affiliated Hospital of Kunming Medical University (Approval No.: KYCS2025-322). Informed consent was obtained from all enrolled patients.

Case acquisition and follow-up procedures involved comprehensive collection of clinical data, including patients' height, weight, parity, menopausal status, human papillomavirus (HPV) status, pathological type of tumor, tumor size, tissue differentiation of tumors, FIGO stage, lymph node metastasis status, surgical procedure, tumor markers (SCC, CA125, CA199, CA153, HE4, and CEA), imaging findings, and phone number. Postoperative follow-up assessments were performed through medical record review and telephone calls from the cancer office until the predetermined study endpoint (December 31, 2024), and progression-free survival (PFS) and overall survival (OS) served as the primary outcome measures. PFS refers to the time from the start of treatment to tumor progression or patient death, whereas OS refers to the time from the start of treatment to patient death due to any cause.

Immunohistochemical Analysis

The immunohistochemical analysis was performed as follows: (1) the tissue sections were deparaffinized in xylene, followed by rehydration in a graded alcohol series; (2) antigen retrieval was performed in citrate buffer in a water bath at 100°C, and the sections were incubated in 3% hydrogen peroxide to block endogenous peroxidase activity; (3) the sections were incubated with the primary antibody (anti-CXCL8, Cat No.: 94407, Cell Signaling Technology) at 20–25°C for 60 min in a dark, humid chamber; (4) a biotinylated secondary antibody and streptavidin–horseradish peroxidase (HRP) conjugate were applied sequentially; (5) and chromogenic development was assessed using DAB substrate and counterstaining with hematoxylin, followed by ethanol dehydration and xylene clearing before mounting with neutral balsam.

The immunohistochemical scores were assessed by two independent pathologists. Staining intensity score was defined as follows: 0, negative; 1, light yellow; 2, tan; and 3, brown. The percentage of positive cells was scored as follows: 0, negative; 1, <10%; 2, 10% −50%; 3, 51%-75%; and 4, >75%. The final immunohistochemical score was calculated as follows: staining intensity score × positive percentage score. Quantitative analysis and immunohistochemical scoring were performed using microscopic examination and ImageJ software.

Enzyme-Linked Immunosorbent Assay

Fresh paired tissue samples (vulvar carcinoma tissue and adjacent normal tissue) were collected, mechanically homogenized, and centrifuged (4°C, 12000 rpm, 15 min). Protein concentrations in the supernatants were quantified using a commercial human IL-8 enzyme-linked immunosorbent assay (ELISA) kit (Cat No.: ECH008, Invitrogen) in accordance with the manufacturer's instructions.

Assessment of Cellular Proliferation

Log-phase cells were harvested, adjusted to a density of 1×10^3 cells/mL in complete medium, and seeded at 1 mL/well in 6-well plates. After overnight incubation in a humidified incubator (37°C, 5% CO_2), cells were treated with recombinant human CXCL8 (0, 80 ng/mL) for 48 h post-treatment, and cell proliferation was evaluated using the EdU Cell Proliferation Kit in SW962 (Cat No.: C0085S, Beyotime) and A431 cells (Cat No.: C0075S, Beyotime) according to the manufacturer's instructions. Images were acquired using a fluorescence microscope (Leica Microsystems, Wetzlar, Germany).

Cell Culture

The human vulvar cancer cell line SW962 was purchased from Zhejiang Meisen Biotechnology Co., Ltd (Hangzhou, China). The human epidermal squamous carcinoma cell line A431 was purchased from Shenzhen Hao Biotechnology Co., Ltd (Guangdong, China). All cell lines were authenticated by short tandem repeat (STR) profiling before experimental use. SW962 cells were cultured in RPMI-1640 medium (Gibco, Grand Island, NY, USA) supplemented with 10% fetal bovine serum (FBS, Vivacell, Shanghai, China), whereas A431 cells were cultured in Dulbecco's modified Eagle

medium (DMEM; Gibco, Grand Island, NY, USA) supplemented with 10% FBS (Vivacell, Shanghai, China). Both cell lines were maintained at 37°C in a 5% CO_2 humidified atmosphere, with medium replacement every 2–3 days and subcultures at 80%–90% confluence using 0.25% trypsin-EDTA solution (Gibco, China).

Cell Cycle Analysis

Cells were seeded into 6-well plates at a density of 1×10^6 cells/mL (1 mL/well) and placed in a humidified 37 °C, 5% CO_2 incubator overnight. After 24 h, the culture medium was aspirated and replaced with fresh medium containing recombinant human CXCL8 at varying concentrations (0, 40, 80, and 200 ng/mL) for 48-h treatment. After incubation, cells were digested into a single-cell suspension using trypsin, and then harvested and fixed in pre-chilled 70% ethanol at 4°C overnight. Cell cycle analysis was then performed according to the manufacturer's instructions (DNA Content Quantitation Assay Kit, Solarbio, Beijing, China) using a flow cytometer with 488-nm laser excitation.

CCK-8 Assay

Vulvar cancer cells in the logarithmic growth phase were digested, counted, and seeded into 96-well plates at a density of 4×10^3 cells per well, with 0.1 mL of complete medium per well. Each concentration condition included at least three replicates. After overnight incubation to ensure cell attachment, the old medium was aspirated and replaced with recombinant CXCL8 protein at gradient concentrations (0, 10, 20, 40, 80, 160, 320, 400, and 800 ng/mL) for 48 h of treatment. After incubation, CCK-8 solution (Cat No.: HY-K0301, MCE) was added under light-protected conditions. The plate was then wrapped in aluminum foil and incubated in the dark for 1–2 h. A microplate reader (Qinxiang, Shanghai, China) was used to measure the absorbance at 450 nm, and the data were analyzed to plot the proliferation curve.

Plate-Clone Formation Assay

After digesting and counting the vulvar cancer cells in the logarithmic growth phase, the cells were seeded into 6-well plates at a density of 8×10^2 cells per well, with 1 mL of complete medium per well. Each concentration condition included at least three replicates. After overnight incubation for cell attachment, the cells were treated with recombinant CXCL8 protein at gradient concentrations (0, 40, 80, 200 ng/mL) for 48 h. The medium was changed periodically over 2–3 days. Cultures were then terminated, and the cells were washed twice with phosphate-buffered saline (PBS), fixed with 4% formaldehyde, and stained with crystal violet solution (0.1%). The images were recorded using a digital camera.

RNA Sequencing Analysis

RNA sequencing was performed using two sets of samples: the vulvar carcinoma tissue and adjacent normal tissue, and the A431 cells treated with vehicle and 200 μM of CXCL8 for 48 h. First, total RNA was extracted using TRIzol reagent kit (Ambi-on, Invitrogen, USA) and its concentration and integrity were determined as previously reported by our group.[20] Then, the RNA samples were sent to Promegene Biotechnology Co., Ltd. (Guangzhou, China) for further processing and analysis.

Quantitative Real-Time Polymerase Chain Reaction

Tissue samples were cut into small pieces and transferred to 1.5-mL Eppendorf tubes containing grinding beads. Next, 1 mL of lysis buffer was added per 50–100 mg tissue, followed by homogenization using a tissue homogenizer. Total RNA was isolated from cells treated with or without esculetin using a RNeasy kit (TIANGEN, Sichuan, China) in accordance with the manufacturer's instructions. cDNA was amplified using a first-strand cDNA synthesis kit (TIANGEN, Sichuan, China) according to the manufacturer's protocol. Semiquantitative polymerase chain reaction (PCR) was performed using gene-specific primers (Table 1). Data were collected using SDS 2.2.2 version, and relative expression was calculated using the $2^{-\Delta\Delta CT}$ method with glyceraldehyde 3-phosphate dehydrogenase (GAPDH) expression serving as the housekeeping control.

Table 1 List of Forward and Reverse Primers Used for Semi-Quantitative PCR

Gene	Forward Primer	Reverse Primer
PI3K	CTTCACAATGCCATCCTACTCC	ATTCAGCCATTCATTCCACCT
TGF-A	GAGAAGCCAGCATGTGTCTGC	ACTCACAGTGCTTCCGGACC
TGF-β	GTTCAGGTACCGCTTCTCGG	CCTGATCGCCTCCCTTCATTT
Smad2	ATGTCGTCCATCTTGCCATTC	AACCGTCCTGTTTTCTTTAGCTT
Smad3	CACGCAGAACGTGAACACC	GGCAGTAGATAACGTGAGGGA-
IL-1β	ATGAAAGACGGCACACCCAC	GGTGCTGATGTACCAGTTGGG
HGF	GGATGGATGGTTAGTTTGAGATACA	CTCTTCCGTGGACATCATGAAT
CTNNB1	TCCCACTCCTACGGAGAGAAA	GAAGGTCGGAAGGAAGG
CXCL8	TTTTGCCAAGGAGTGCTAAAG	AACCCTCTGCACCCAGTTTTC
CXCL1	CAAACCGAAGTCATAGCCACA	CTCCTAAGCGATGCTCAAACA
CXCL5	ACAGACCACGCAAGGAGTT	TCTTCAGGGAGGCTACCAC
CXCR2	CTGCCTGTCTTACTTTTCC	CAGTTTGCTGTATTGTTGC
VEGF	GAGGAGTCCAACATCACC	TGTCTTGCTCTATCTTTCTTT
E-cadherin	ACGCATTGCCACATACA	CGTTAGCCTCGTTCTCA
Vimentin	ATGGCTCGTCACCTTCG	AGTTTCGTTGATAACCTGTCC
Slug	AGCAGTTGCACTGTGATGCC	ACACAGCAGCCAGATTCCTC
Nanog	AATGGTGTGACGCAGGGATG	TGCACCAGGTCTGAGTGTTC
TGFBR1	CCTCGAGATAGGCCGTTTGT	GCAATGGTAAACCAGTAGTTGGA
MMP-2	TGCTGAAGGACACACTAAAGAAGATG	GCTTGCGAGGGAAGAAGTTGTAG
MMP-9	CGAACTTTGACAGCGACAAGAA	CGGCACTGAGGAATGATCTAAGC
18S	AACCCGTTGAACCCCATT	CCATCCAATCGGTAGTAGCG
IL-4	GTGACGGTGTTGATGGTAAGAT	TACATGATCACACAAAAGCACG
MSMO1	GTTCATCATGAGTTTCAGGCTC	TACATGATCACACAAAAGCACG
miR-26	CCTCGGCCTGGTTCAAGTAA	GGCCACTTCCTGACACAAGTA
REGY	CGAACGGTACAAATGCCAGT	CACAAACGACCAGCCACAAG
US	CAACAGGCTCGTGAAAGACC	GTTCGTCAACCTAGCGCAG
CCL2	GTCTGTGCTGACCCCAAGAA	AAGGCA TCACAGTCCGAGTC
CCR2	GCT GTGTTTGCCTCTCTACCAG	CAAGTAGAGGCAGGATCAGGCT
FoxM1	GCGACAGGTTAAGGTTGAC	AGGTTGTGGCGGATGGAGT
GAPDH	AAAGGGTCATCATCTCTG	GCTGTTGTCATACTTCTC

Tumor Xenograft Assay

Twelve female BALB/c nude mice aged 6–8 weeks were purchased from Spivey (Beijing) Biotechnology Co. and maintained in a specific pathogen-free laboratory animal building at the Institute of Medical Biology of the Chinese Academy of Medical Sciences. After one week of acclimatization, the nude mice were randomly divided into two groups according to body weight and received subcutaneous injection of A431 vulvar cancer cells (5×10^6 cells/mouse). From the second day, the experimental mice received injections containing 100 μL of 0.9% normal saline or 200 ng/mL of recombinant CXCL8 protein solution through the tail vein every three days. The body weights and tumor volumes of the mice were measured daily during the treatment period. The tumor volume was calculated using the following formula: tumor volume = length × width^2/2. After 12 days, mice were sacrificed by cervical dislocation, followed by tumor excision, weighing, and imaging for further analysis. All procedures were approved by the Animal Ethics Committee of Kunming Medical University (Approval No.: kmmu20231049). All animal housing and experiments were conducted in strict accordance with the institutional guidelines for care and use of laboratory animals.

Statistical Analysis

Protein expression levels were quantified using ImageJ software, whereas cell cycle distribution profiles were analyzed using ModFit-1 software. Data visualization was performed using GraphPad Prism 8.0 (GraphPad Software), and statistical analyses were conducted using SPSS 26.0 (IBM Co). Patient survival status was analyzed using the

Kaplan–Meier test. All experiments were independently repeated at least three times. All data were tested for normality, and the results were expressed as mean ± standard deviation (SD). Statistical significance was determined using *t*-tests, one-way or two-way analysis of variance (ANOVA), or rank-sum tests, as appropriate. $P<0.05$ was considered statistically significant (*$P < 0.05$; **$P < 0.01$; ***$P < 0.001$).

Results

CXCL8 Expression Was Significantly Upregulated in Vulvar Cancer Tissues in Comparison Adjacent Normal Tissues

To identify genes associated with vulvar cancer, RNA sequencing was performed on five paired samples of vulvar cancer tissues and adjacent normal tissues to detect differentially expressed genes (DEGs). Comparative analysis revealed 1,644 significantly upregulated and 2,807 down-regulated genes (Figure 1A). Hierarchical clustering analysis of these DEGs demonstrated distinct gene expression patterns, as visualized in the heatmap (Figure 1B). Next, the expression levels of CXCL8 in vulvar cancer and adjacent normal tissues were further validated by ELISA and immunohistochemical analyses (Figure 1C and D). Consistent with the RNA sequencing results, the expression of CXCL8 was significantly upregulated in vulvar cancer tissues in comparison with adjacent normal tissues.

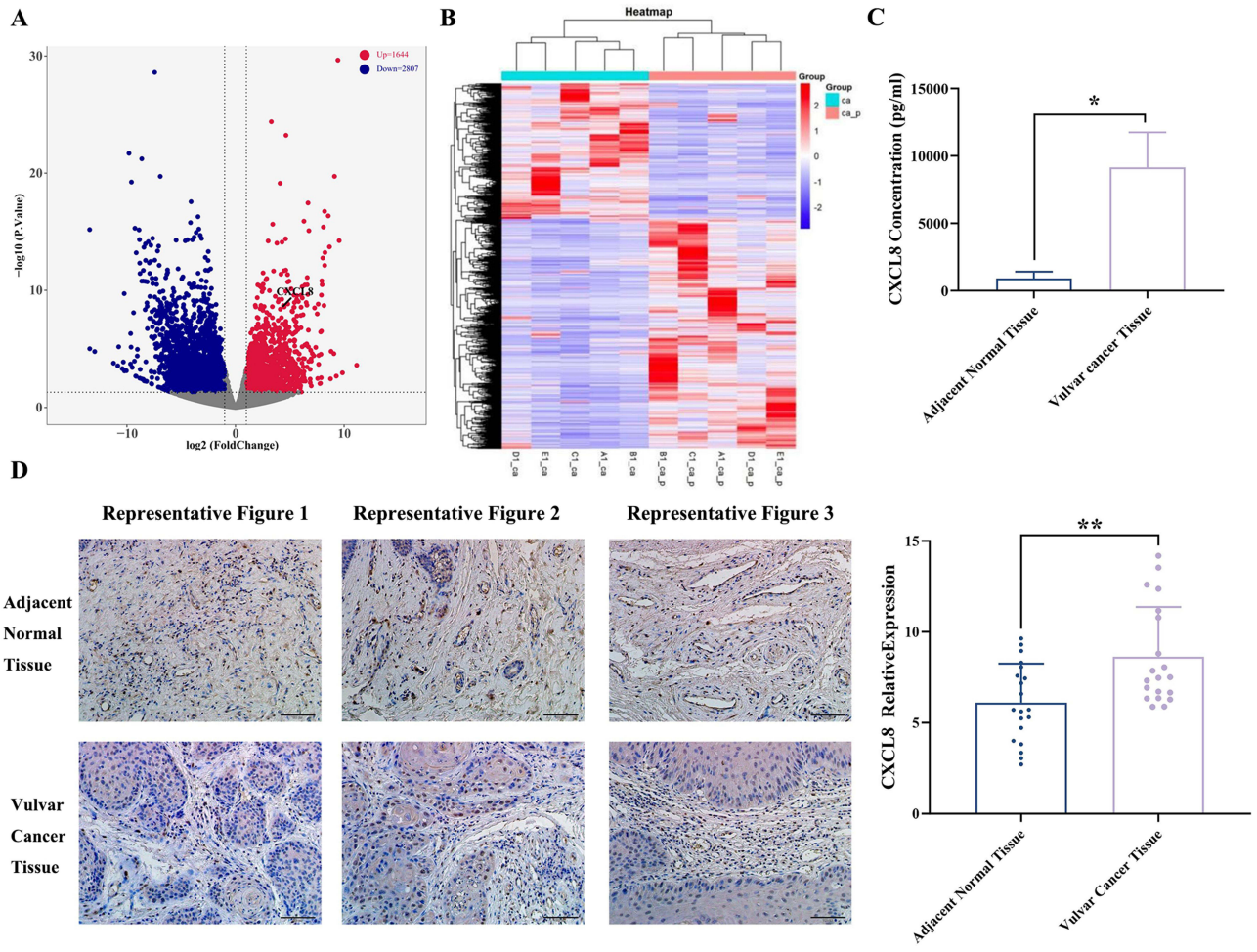

Figure 1 CXCL8 expression was significantly upregulated in vulvar cancer tissues in comparison with adjacent normal tissues. (**A**) Volcano plot illustrating DEGs between vulvar cancer tissues and paired adjacent normal tissues (n = 5 pairs). (**B**) Heatmap. (**C**) Tissue CXCL8 concentrations determined by ELISA; data are presented as mean ± SD, *$P < 0.05$, paired Student's *t*-test. (**D**) Representative immunohistochemical staining of CXCL8 in VSCC and adjacent non-tumor tissues (scale bar, 100 μm, 20×) with corresponding integrated optical density (IOD) quantification. The three images above are three representative images from the "Adjacent normal tissue" group, whereas the three images below are three representative images from the "Vulvar cancer tissue" section. Data are presented as mean ± SD, **$P < 0.01$, paired Student's *t*-test.

CXCL8 Promoted the Proliferation of Vulvar Cancer Cells

To assess the proliferative effects of CXCL8 on vulvar cancer cells, we conducted CCK-8, plate-clone formation, and 5-ethynyl-2′-deoxyuridine (EdU) staining assays. CCK-8 assays demonstrated that the optical density (OD) values for both SW962 and A431 cells increased in a concentration-dependent manner upon treatment with recombinant human CXCL8 for 48 h (Figure 2A and B).

The plate-clone formation assay revealed that recombinant human CXCL8 enhanced clone-formation ability in both SW962 and A431 cells. For SW962 cells, clone numbers increased from 90 (control) to 156, 257, and 397 following treatment with 10, 40, and 80 ng/mL recombinant human CXCL8, respectively (Figure 2C and D). Similarly, A431 cells showed elevated clone numbers from 137 (control) to 170, 184, and 226 at the corresponding recombinant human CXCL8 concentrations (Figure 2C and E).

EdU staining assays also indicated that the ratio of EdU-positive cells for both SW962 and A431 cells was significantly greater after the treatment with recombinant human CXCL8 (Figure 2F). These findings suggest that upregulation of CXCL8 could promote the proliferation of vulvar cancer cells.

CXCL8 Alters the Cell Cycle Progression of Vulvar Cells

To elucidate the mechanisms underlying the potential proliferative effects of recombinant human CXCL8 in SW962 and A431 vulvar cancer cells, cell cycle distribution was assessed by flow cytometry. Our results demonstrated that exposure to recombinant human CXCL8 reduced the number of SW962 and A431 cells in the G0/G1 phase and increased the proportion of cells in the S and G2/M phases in a concentration-dependent manner (Figure 3A–C).

CXCL8 Promotes the Growth of VSCC in vivo

After establishment of the cell line-derived xenograft (CDX) model in BALB/c nude mice, the pro-tumor effect of recombinant human CXCL8 was evaluated by tail administration. The results showed that tumor-growth ability in recombinant human CXCL8-treated mice was greater than that in controls (Figure 4A and B), with increased tumor volumes observed in the treatment group (Figure 4C). Notably, the two groups showed no significant differences in body weight (Figure 4D). Furthermore, the expression levels of vascular endothelial growth factor (VEGF) and Ki-67 were both upregulated following CXCL8 treatment (Figure 4E).

Transcriptome Analysis of A431 Cells Treated with Recombinant Human CXCL8 and Verification of the Expression Levels of DEGs

RNA sequencing of recombinant human CXCL8-treated A431 cells revealed significant activation of the transforming growth factor (TGF-β)-signaling pathway, with >1000 DEGs (Figure 5A–D). Quantitative real-time (qRT)-PCR was used to validate the most altered DEGs. The results showed that the mRNA expression levels of matrix metalloproteinase 9 (MMP9; $P < 0.001$), TGF-β ($P < 0.01$), and PI3K ($P < 0.001$) were statistically significant, consistent with the RNA-seq results (Figure 5E and F). Thus, a strong transcriptional response was observed after recombinant human CXCL8 treatment.

Correlation Between the Expression of CXCL8 and Clinicopathological Features in Patients with Vulvar Cancer

After stratifying patients with VSCC into CXCL8-high and CXCL8-low groups on the basis of validated immunohistochemical scoring, the correlations between CXCL8 expression and clinicopathological characteristics were analyzed. The results revealed that follow-up outcomes ($P = 0.0142$) and tumor size ($P = 0.0142$) were significantly correlated with the expression of CXCL8 levels. In contrast, no statistically significant correlations were found with body mass index (BMI), parity, menopausal status, HPV infection status, tissue differentiation of tumors, FIGO stage, surgical procedure, and lymph node metastasis (Table 2).

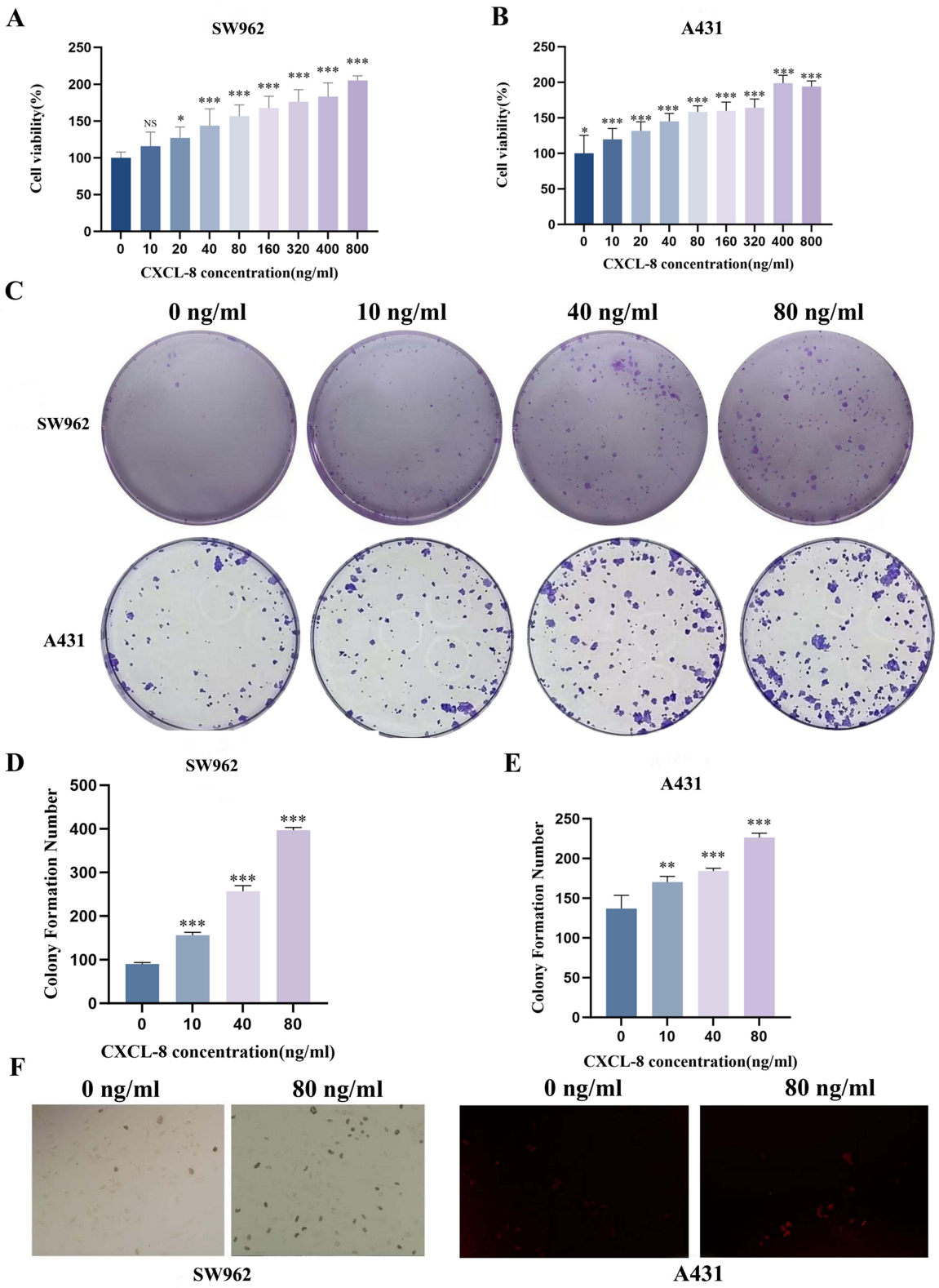

Figure 2 Recombinant human CXCL8 promotes proliferation of VSCC cells. (**A** and **B**) CCK-8 assays for SW962 (**A**) and A431 (**B**) cells. Data are presented as mean ± SD from three independent experiments; **P* < 0.05, ****P* < 0.001 vs. 0 ng/mL (ANOVA followed by Dunnett's test). (**C**) Representative images of the findings from colony-formation assays for SW962 and A431 cells. (**D** and **E**) Quantification of colony numbers for SW962 (**D**) and A431 (**E**) cells; data are presented as mean ± SD of triplicate wells; ***P* < 0.01, ****P* < 0.001, Student's *t*-test. (**F**) EdU staining assays were performed to determine the proliferation in SW962 and A431 cells treated with 0 or 80 ng/mL CXCL8 for 48 h. Images were acquired at 200× magnification; scale bar, 100 μm.

https://doi.org/10.2147/IJWH.S569683

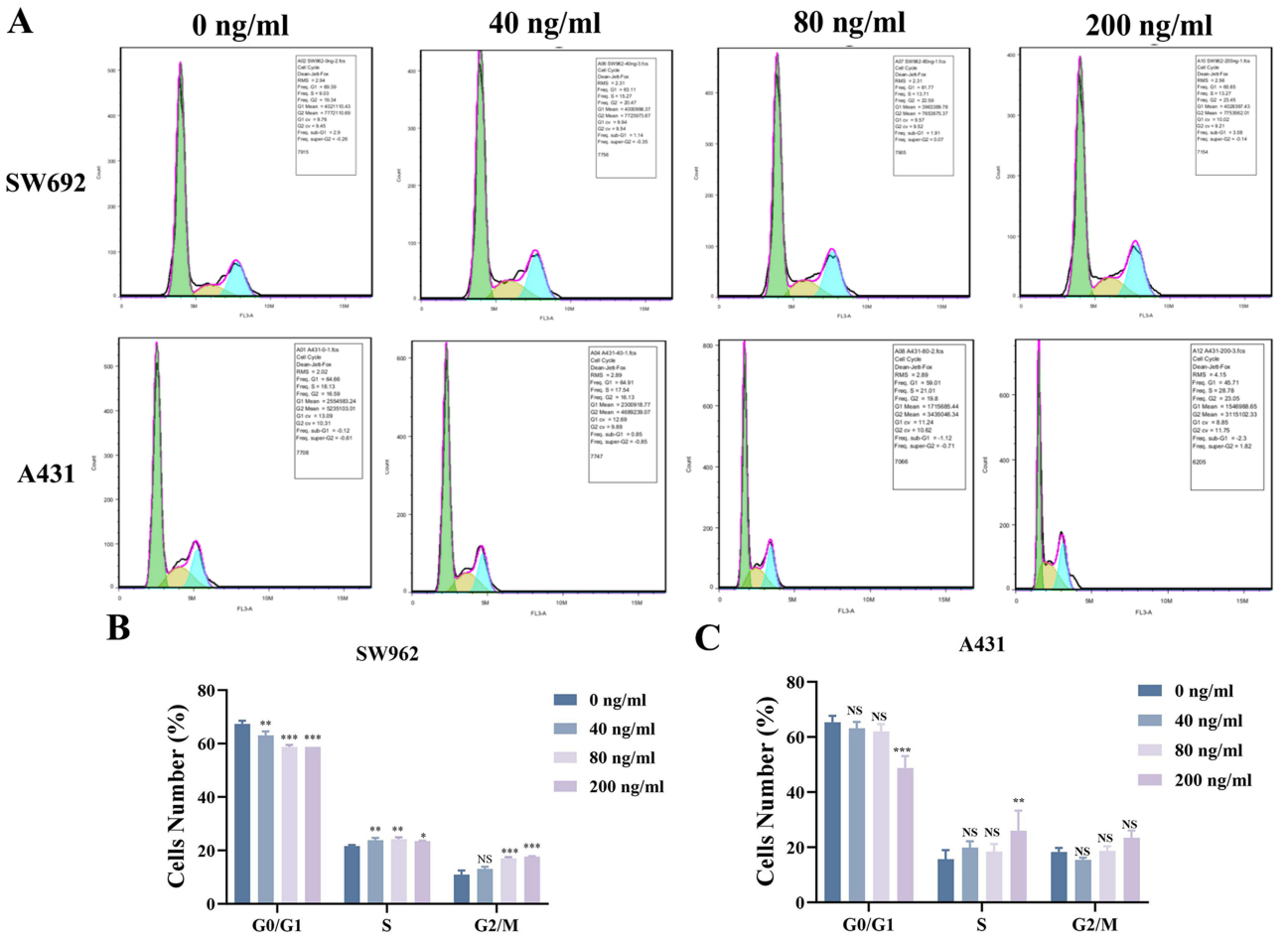

Figure 3 Recombinant human CXCL8 alters the cell cycle progression in vulvar carcinoma cells. (**A**) Flow cytometry histograms. (**B** and **C**) Quantification of cell cycle distribution in SW962 cells (**B**) and A431 cells (C). Data are presented as mean ± SD from three independent experiments; *P < 0.05, **P < 0.01, ***P < 0.001 vs. 0 ng/mL (one-way ANOVA followed by Dunnett's test).

Effects of CXCL8 Expression on PFS and OS in Patients with Vulvar Cancer

A retrospective analysis of 60 patients s with VSCC evaluated the prognostic value of CXCL8 expression on the basis of immunohistochemical scoring. Patients were stratified into CXCL8-low (n = 31) and CXCL8-high (n = 29) groups. Survival analyses using PFS and OS as endpoints revealed that the CXCL8-high group had a median PFS of 58 months, whereas the median PFS of the CXCL8-low group was undefined due to insufficient follow-up data. A statistically significant difference in PFS was observed between the groups (P = 0.0011), demonstrating that high CXCL8 expression correlates with worse PFS (Figure 6A).

At the follow-up cutoff date (December 31, 2024), follow-up cutoff date, 21 deaths (35.0%) had occurred in the cohort. Kaplan-Meier analysis revealed significantly worse OS in CXCL8-high group versus the CXCL8-low group (P = 0.013), indicating that elevated CXCL8 expression is an important predictor of poorer OS (Figure 6B).

Discussion

In the present study, we focused on two core directions. First, we systematically evaluated the correlation between the expression levels of CXCL8 and the prognosis as well as the clinicopathological characteristics of patients with vulvar cancer, revealing the clinical prognostic value of CXCL8 as a potential biomarker. Second, we elucidated the molecular mechanisms by which CXCL8 promotes the occurrence and progression of vulvar cancer through regulation of malignant biological behaviors such as proliferation, thereby providing a theoretical basis for the development of targeted therapies.

https://doi.org/10.2147/IJWH.S569683

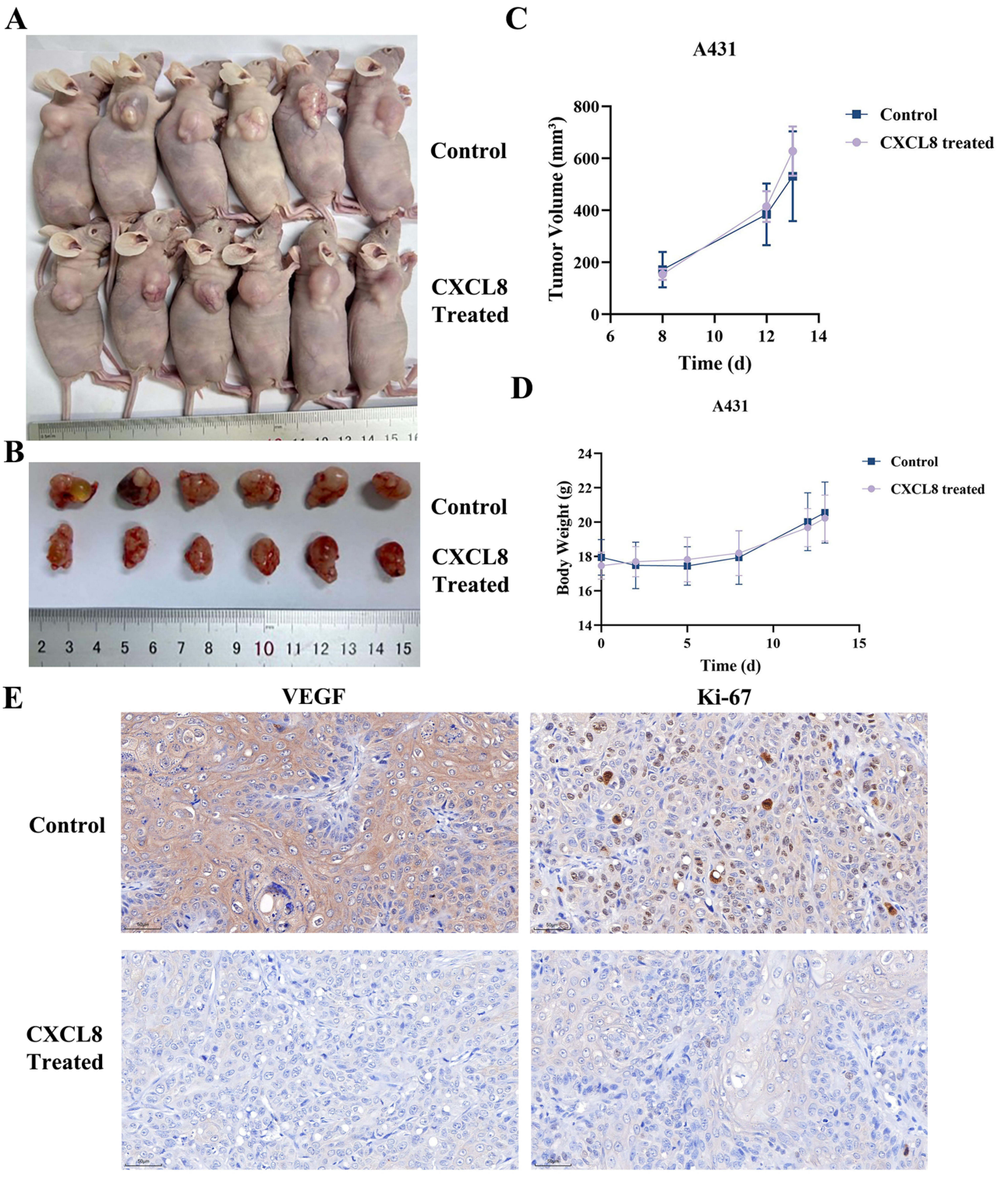

Figure 4 CXCL8 promotes tumor growth in a xenograft mouse model of VSCC. (**A** and **B**) Images of BALB/c nude mice (**A**) and tumor morphology (**B**) at the end of the experiment after tumor formation in control and CXCL8-treated groups. (n=6 per group). (**C**) Tumor volume measurements over 14 days; data are presented as mean ± SD. The groups showed no significant differences. (**D**) Body weight of mice over the course of the experiment; data are presented as mean ± SD. No significant differences were observed between groups. (**E**) Immunohistochemical staining for VEGF and Ki-67 expression in tumor sections from control and CXCL8-treated groups. Scale bar, 50 μm, ×400.

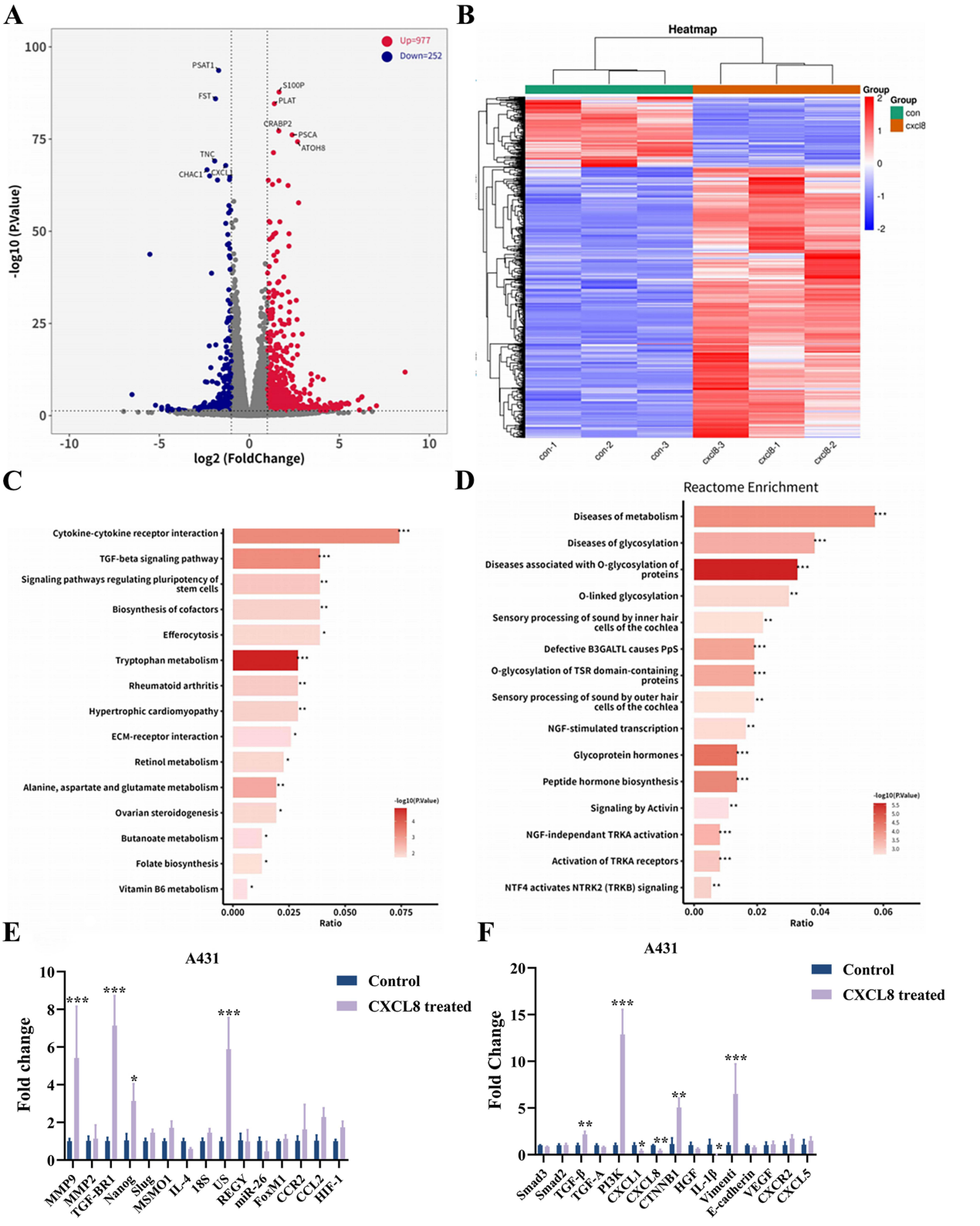

Figure 5 Recombinant human CXCL8 promotes tumor progression through the CXCL8/TGF-β axis in A431 cells. (**A**) Volcano plot showing DEGs in A431 cells treated with 200 ng/mL CXCL8 for 48 h in comparison with the control (0 ng/mL). (**B**) Heatmap of hierarchical clustering for the top 50 DEGs. (**C**) Bar plot depicting the top 15 enriched pathways from the DEGs. **P* < 0.05, ***P* < 0.01, ****P* < 0.001 vs. control. (**D**) Reactome enrichment analysis of the DEGs. ***P* < 0.01, ****P* < 0.001 vs. control. (**E**) qRT-PCR validation of selected DEGs (MMP9, MMP2, TGF-BR1 et al) in A431 cells treated with 200 ng/mL CXCL8 for 48 h; data are presented as mean ± SD from three independent experiments; **P* < 0.05, ****P* < 0.001 vs. control (Student's *t*-test). (**F**) qRT-PCR validation of selected DEGs (Smad3, Smad2, TGF-β et al) in A431 cells treated with 200 ng/mL CXCL8 for 48 h; data are presented as mean ± SD from three independent experiments; **P* < 0.05, ***P* < 0.01, ****P* < 0.001 vs. control (Student's *t*-test).

https://doi.org/10.2147/IJWH.S569683

Table 2 Correlation Between CXCL8 Expression and Clinicopathological Characteristics of Vulvar Cancer Patients

Characteristic	CXCL8		*P* Value
	Low Expression	High Expression	
BMI (kg/m^2)			0.672
<28	27 (12.90%)	27 (6.90%)	
≥28	4 (87.10%)	2 (93.10%)	
Menopausal status			0.573
Postmenopausal	21 (67.74%)	22 (75.86%)	
Premenopausal	10 (32.26%)	7 (24.14%)	
Number of deliveries			0.465
≥2 times	28 (90.32%)	24 (82.76%)	
<2 times	3 (9.68%)	5 (17.24%)	
HPV infection status			>0.99
HPV-positive	4 (12.90%)	3 (10.34%)	
HPV-negative or unknown	27 (87.10%)	26 (89.66%)	
Tumor size			0.0142
≤4cm	15 (33.33%)	5 (13.89%)	
>4cm	16 (66.67%)	24 (86.11%)	
Histological differentiation			0.7737
Well-differentiated	22 (70.97%)	22 (75.86%)	
Moderately/Poorly-differentiated	9 (29.03%)	7 (24.14%)	
FIGO stage			0.1173
Stage I	21 (67.74%)	13 (44.83%)	
> Stage I	10 (32.26%)	16 (55.17%)	
Lymph node metastasis			0.3545
Present	5 (16.13%)	8 (27.59%)	
Absent	26 (83.87%)	21 (72.41%)	
Surgical approach			0.509
Radical vulvectomy	7 (22.58%)	4 (13.79%)	
Radical vulvectomy + inguinal lymphadenectomy ± pelvic lymphadenectomy	24 (77.42%)	25 (86.21%)	
Follow-up outcome			0.0142
Alive	25 (80.65%)	14 (48.28%)	
Deceased	6 (19.35%)	15 (51.72%)	

Previous studies have demonstrated CXCL8 overexpression in multiple malignancies.[21] Highly CXCL8 expression plays an important role in the occurrence, development, metastasis, and immune evasion of various tumors (such as gastric cancer, colon carcinoma, breast cancer, and ovarian cancer), promoting tumor proliferation and resulting in poor prognoses

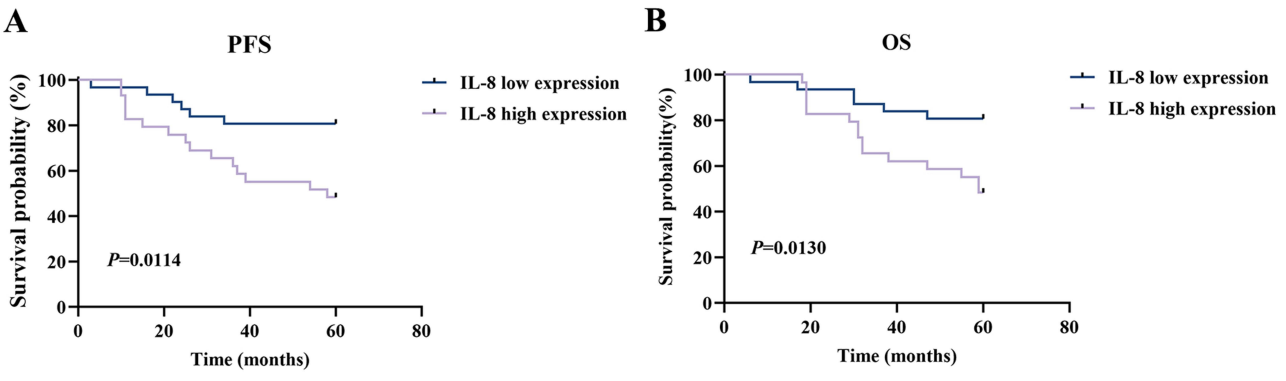

Figure 6 Influence of CXCL8 expression on survival outcomes in patients with VSCC. (**A**) Kaplan–Meier curve for PFS showing a significant difference between the low (n = 31) and high (n = 29) CXCL8 expression groups, *P* = 0.0011. (**B**) Kaplan–Meier curve for OS demonstrating poorer OS in the high CXCL8 expression group than in the low expression group, *P* = 0.0130.

in patients with cancer.[22–24] Simultaneously, the correlation between high CXCL8 expression levels and the prognosis and clinical features of tumors was also explored, which is supposed to be associated with increased tumor malignancy, enhanced metastatic potential, and poor prognosis.[25–27] A total of 60 patients with VSCC who underwent surgical treatment for the first time were included in this study. Paraffin-embedded tissue specimens were subjected to immunohistochemical analysis, and the corresponding clinical cases were retrospectively analyzed. The findings of our study revealed that patients with high CXCL8 expression exhibited shorter PFS and overall survival OS than those with low CXCL8 expression, indicating that high CXCL8 expression is associated with a poor prognosis. This discovery aligns closely with the conclusions from multiple previous studies demonstrating that elevated CXCL8 expression predicts adverse outcomes. For example, in non-small cell lung cancer, patients with high CXCL8 expression exhibit significantly higher rates of lymph node metastasis and advanced-stage disease occurrence, and CXCL8 serves as an independent predictor of these outcomes while functioning as a potential biomarker for evaluating five-year survival rates.[28] For gastric cancer, Zhai et al reported that IL-8 secreted by gastric cancer cells enhances the chemotherapy resistance of tumor cells, resulting in a poor patient prognosis. Moreover, immunohistochemical analysis of gastric cancer tissues from chemotherapy-resistant patients showed abnormal CXCL8 expression levels and localization, and high serum CXCL8 concentrations were closely related to poor response to cisplatin treatment in patients.[29] Additionally, serum CXCL8 concentrations have also been demonstrated to accurately reflect the tumor burden following antitumor therapy in other malignant tumors such as melanoma and refractory pancreatic carcinoma.[30–32] In summary, both our study and previous explorations of other cancer types showed that high expression of CXCL8 is closely related to tumor progression, treatment resistance, and poor prognosis, fully demonstrating the potential value of CXCL8 as a prognostic indicator for tumors. Furthermore, in the present study, no significant association was found between CXCL8 expression level and HPV infection status in patients with vulvar cancer. We believe that this was partly due to the fact that some of the included patients did not undergo HPV testing and the number of cases with HPV infection included in the statistical analysis was insufficient. Therefore, this aspect needs to be studied further by expanding the sample size through multi-center collaboration.

The proliferation and angiogenesis of tumors play critical roles in tumor progression and metastasis. Previous studies have certified that CXCL8 can induce the proliferation of triple-negative breast cancer, colorectal cancer, lung cancer, and ovarian cancer cells by activating signaling pathways such as the PI3K/AKT, MAPK, nuclear factor (NF)-κB, and Wnt/β-catenin pathways. CXCL8 has also been shown to activate corresponding pathways to promote the proliferation and migration of pancreatic carcinoma, neuroglioma, and vascular endothelial cells, facilitating angiogenesis and tumor growth.[33–36] Inhibition of CXCL8 also leads to impaired tumor vascularization and tumor death. To further investigate whether CXCL8 is involved in regulating the malignant biological behaviors of vulvar cancer cells, we treated the vulvar cancer cell lines SW962 and A431 with different concentrations (0, 40, 80, 200 ng/mL) of recombinant human CXCL8 and obtained an important finding: CXCL8 can promote the proliferation of A431 and SW962 vulvar cancer cells and facilitates the transition of the cell cycle from the G0/1 phase to the S phase. Using the A431 xenograft nude mouse model, the results further confirmed that tail vein injection of recombinant human CXCL8 significantly accelerated tumor growth and induced obvious angiogenesis; immunohistochemical analysis showed that both Ki-67 and VEGF expression were significantly upregulated in the CXCL8-treated group. These results are highly consistent with previously reported findings showing that CXCL8 promotes gastric cancer proliferation and migration, and that the CXCL8/CXCR2 axis drives angiogenesis in endothelial cells in glioblastoma.[37,38] Notably, previous studies have shown that sunitinib inhibits angiogenesis in renal cell carcinoma by blocking VEGF/platelet-derived growth factor (PDGF) receptors, whereas CXCL8 overexpression can lead to drug resistance; blocking CXCL8 signaling can restore sensitivity to sunitinib.[39] These studies collectively suggest that CXCL8 is a key regulatory factor in the vascular microenvironment of multiple tumors. With our in vivo experimental data, CXCL8 can be inferred to similarly promote the malignant progression of vulvar cancer by inducing angiogenesis and cell proliferation, and may serve as an important target for predicting prognosis and reversing drug resistance.

To investigate the potential mechanisms by which CXCL8 promotes tumor cell proliferation, we employed transcriptome sequencing and Kyoto Encyclopedia of Genes and Genomes (KEGG) enrichment analysis of vulvar cancer cells treated with CXCL8 for 48 h. The results indicated significant enrichment in signaling pathways in CXCL8-treated vulvar cancer cells, such as the EMT and TGF-β pathways. EMT is the process by which epithelial cells transform into

a mesenchymal phenotype, and it commonly occurs in biological processes such as tissue repair, tumor invasion, and metastasis. TGF-β is the most critical mediator in epithelial cell proliferation and EMT. TGF-β has been reported to significantly reduce the proliferation of oral squamous cell carcinoma cells in vitro and participates in the occurrence of EMT, consistent with our findings.[40] Therefore, we preliminarily hypothesize that CXCL8 in vulvar cancer cells may promote disease progression through the TGF-β pathway.

Our study established CXCL8 as both a prognostic biomarker and a promising therapeutic target for inhibiting tumor proliferation in vulvar cancer. Moreover, the findings highlight TGF-β as a critical downstream signaling mediator in this pathway.

Conclusion

To the best of our knowledge, this is the first study to demonstrate the predictive value of the CXCL8 expression level in the prognosis of vulvar cancer patients and to explore the role of CXCL8 in vulvar cancer in vitro and in vivo. Our results show that patients with vulvar cancer and high CXCL8 expression have a poor prognosis; cell experiments revealed that CXCL8 not only promotes the proliferation of vulvar cancer but also induces the cell cycle to shift to the S and G2/M phases in vitro; moreover, tail vein injections of CXCL8 promoted tumor growth in a xenograft mouse model of vulvar cancer. Notably, our results initially revealed that the mechanism by which CXCL8 promotes vulvar cancer was closely related to the activation of TGF-β signaling pathway. Taken together, these findings suggest that CXCL8 may serve as a therapeutic target for vulvar cancer.

Abbreviations

VSCC, Vulvar squamous cell carcinoma; CXCL8, C-X-C motif chemokine ligand 8; GEO, Gene Expression Omnibus; EMT, Epithelial-mesenchymal transition.

Data Sharing Statement

The datasets generated and analyzed during the current study are available from the corresponding author Professor Hongping Zhang upon reasonable request.

Ethics Approval and Consent to Participate

The animal experiment protocol has been reviewed and approved by the Animal Ethics Committee of Kunming medical University and the approved number is kmmu20231049. This human study complied with the Declaration of Helsinki and was approved by the Human Ethics Committee of Yunnan cancer hospital (KYCS2025-322). The informed consent was obtained from all enrolled subjects.

Acknowledgments

We sincerely thank Cancer Institute of Yunnan Province providing the scientific research platform for us.

Author Contributions

All authors made a significant contribution to the work reported, whether that is in the conception, study design, execution, acquisition of data, analysis and interpretation, or in all these areas; took part in drafting, revising or critically reviewing the article; gave final approval of the version to be published; have agreed on the journal to which the article has been submitted; and agree to be accountable for all aspects of the work.

Funding

This work was supported by grants from Basic Research in Yunnan Province (Kunming Medical University Joint Project): 202401AY070001-043. The innovative research team of Yunnan Province (Project Number: 202305AS350020). The Innovation and Entrepreneurship Training Program for College Students of Kunming Medical University (Grant No.: 2024CYD053), Yunnan Provincial Department of Science and Technology (Grant No.: 202101BA070001-001). "Xingdian Talent Support Plan" for Outstanding Doctors in Yunnan Province (Project Number: XDYC-MY-2022-0056).

Disclosure

Xing-Yan Wu, Yong-Jun Zhang and Jing-Man Li are co-first authors for this study. The authors declared that they have no conflicts of interest regarding this work.

References

1. Abu-Rustum NR, Yashar CM, Arend R, et al. Vulvar cancer, Version 3.2024, NCCN clinical practice guidelines in oncology. *J Natl Compr Canc Netw*. 2024;22:117–135. doi:10.6004/jnccn.2024.0013
2. Bray F, Laversanne M, Sung H, et al. Global cancer statistics 2022: GLO-BOCAN estimates of incidence and mortality worldwide for 36 cancers in 185 countries. *CA Cancer J Clin*. 2024;74:229–263. doi:10.3322/caac.21834
3. Siegel RL, Kratzer TB, Giaquinto AN, Sung H, Jemal A. Cancer statistics, 2025. *CA Cancer J Clin*. 2025;75:10–45. doi:10.3322/caac.21871
4. Oonk MHM, Planchamp F, Baldwin P, et al. European Society of Gynaecological Oncology guidelines for the management of patients with vulvar cancer - update 2023. *Int J Gynecol Cancer*. 2023;33:1023–1043. doi:10.1136/ijgc-2023-004486
5. Board PDQATE. Vulvar Cancer Treatment (PDQ®): patient Version. In: *PDQ Cancer Information Summaries*. Bethesda (MD): National Cancer Institute (US); 2002.
6. Lukovic J, Han K. Postoperative management of vulvar cancer. *Int J Gynecol Cancer*. 2022;32:338–343. doi:10.1136/ijgc-2021-002463
7. Caretto AA, Servillo M, Tagliaferri L, et al. Sec-ondary post-oncologic vulvar reconstruction - a simplified algorithm. *Front Oncol*. 2023;13:1195580. doi:10.3389/fonc.2023.1195580
8. Domingues AP, Mota F, Durão M, Frutuoso C, Amaral N, de Oliveira CF. Neoadjuvant chemotherapy in advanced vulvar cancer. *Int J Gynecol Cancer*. 2010;20:294–298. doi:10.1111/igc.0b013e3181c93adc
9. Vicente-Pardo A, Anderssen Lorca B, Sanchez-Garcia A, Vicente-Pardo P, Pérez-García A. Reconstruction of a large thoracic radiation-induced ulcer using a free extended vertical rectus abdominis myocutaneous flap. *Plast Aesthet Nurs*. 2022;42:66–68. doi:10.1097/psn.0000000000000423
10. Dobrică EC, Vâjâitu C, Condrat CE, et al. Vulvar and vaginal melanomas-the darker shades of gynecological cancers. *Biomedicines*. 2021;9:758. doi:10.3390/biomedicines9070758
11. Deng F, Weng Y, Li X, Wang T, Fan M, Shi Q. Overexpression of IL-8 promotes cell migration via PI3K-Akt signaling pathway and EMT in triple-negative breast cancer. *Pathol Res Pract*. 2021;223:152824. doi:10.1016/j.prp.2020.152824
12. Meng ZW, Zhang L, Cai XR, Wang X, She FF, Chen YL. IL-8 is a novel prometastatic chemokine in intrahepatic cholangiocarcinoma that induces CXCR2-PI3K/AKT signaling upon CD97 activation. *Sci Rep*. 2023;13:18711. doi:10.1038/s41598-023-45496-3
13. Chen F, Aye L, Yu L, et al. SSH1 promotes progression of intrahepatic cholangiocarcinoma via p38 MAPK-CXCL8 axis. *Carcinogenesis*. 2023;44:232–241. doi:10.1093/carcin/bgad009
14. Sun F, Wang J, Sun Q, et al. Interleukin-8 promotes integrin β3 upregulation and cell invasion through PI3K/Akt pathway in hepatocellular carcinoma. *J Exp Clin Cancer Res*. 2019;38:449. doi:10.1186/s13046-019-1455-x
15. Huang Y, Hong W, Wei X. The molecular mechanisms and therapeutic strategies of EMT in tumor progression and me-tastasis. *J Hematol Oncol*. 2022;15:129. doi:10.1186/s13045-022-01347-8
16. Lin W, Li S, Meng Y, et al. UDCA inhibits hypoxic hepatocellular carcinoma cell-induced angiogenesis through suppressing HIF-1α/VEGF/IL-8 intercellular signaling. *Front Pharmacol*. 2021;12:755394. doi:10.3389/fphar.2021.755394
17. Zhang N, Pang C, Li Z, Xu F, Zhao L. Serum CXCL8 and CXCR2 as diagnostic biomarkers for noninvasive screening of cervical cancer. *Medicine*. 2023;102:e34977. doi:10.1097/md.0000000000034977
18. Lin L, Li L, Ma G, Kang Y, Wang X, He J. Overexpression of IL-8 and Wnt2 is associated with prognosis of gastric cancer. *Folia Histochem Cytobiol*. 2022;60:66–73. doi:10.5603/FHC.a2022.0002
19. Yan X, Han L, Zhao R, Fatima S, Zhao L, Gao F. Prognosis value of IL-6, IL-8, and IL-1β in serum of patients with lung cancer: a fresh look at interleukins as a biomarker. *Heliyon*. 2022;8:e09953. doi:10.1016/j.heliyon.2022.e09953
20. Yang X, Liu Z, Wang X, et al. Anti-cancer effects of nitazoxanide in epithelial ovarian cancer in-vitro and in-vivo. *Chem Biol Interact*. 2024;400:111176. doi:10.1016/j.cbi.2024.111176
21. Fu X, Wang Q, Du H, Hao H. CXCL8 and the peritoneal metastasis of ovarian and gastric cancer. *Front Immunol*. 2023;14:1159061. doi:10.3389/fimmu.2023.1159061
22. Ma YT, Zheng L, Zhao CW, et al. Interferon-α induces differentiation of cancer stem cells and immunosuppression in hepatocellular carcinoma by upregulating CXCL8 secretion. *Cy-tokine*. 2024;177:156555. doi:10.1016/j.cyto.2024.156555
23. Ren M, Chen LL, Jiang LY, Yu HH, Ji HZ. The CXCL8-CXCR2 axis promotes M2 macrophage polarization in ovarian cancer via RASGRP4-mediated mTOR-STAT3 signaling. *Apoptosis*. 2025;30:1839–1851. doi:10.1007/s10495-025-02128-7
24. Zhai C, Ye J, Zhou Z, et al. Bioinformatics analysis identifies NT5M modulates immune evasion through PD-L1 via CXCL8 in pancreatic adenocarcinoma. *Sci Rep*. 2025;15:26207. doi:10.1038/s41598-025-10098-8
25. Hutajulu SH, Astari YK, Paramita DK, et al. High IL-8 plasma levels at baseline are predictive of poor overall survival in breast cancer patients receiving chemotherapy. *BMC Res Notes*. 2025;18:283. doi:10.1186/s13104-025-07353-6
26. Łukaszewicz-zając M, Pączek S, Mroczko P, Kulczyńska-Przybik A. The significance of CXCL1 and CXCL8 as well as their specific receptors in colorectal cancer. *Cancer Manag Res*. 2020;12:8435–8443. doi:10.2147/cmar.S267176
27. Ma X, Zhu X, Zou M, et al. Expression of CXCL8 and its relationship with prognosis in patients with non-small cell lung cancer. *Am J Cancer Res*. 2024;14:2934–2945. doi:10.62347/ljdq3897
28. Zou W, Hu TH. Effect of chemokine interleukin-8, monocyte chemoattractant protein-1 and macrophage inflammatory protein-1 on the angiogenesis of non-small cell lung cancer. *Zhong Nan Da Xue Xue Bao Yi Xue Ban*. 2007;32:665–670.
29. Zhai J, Shen J, Xie G, et al. Cancer-associated fibroblasts-derived IL-8 mediates resistance to cisplatin in human gastric cancer. *Cancer Lett*. 2019;454:37–43. doi:10.1016/j.canlet.2019.04.002
30. Merz V, Zecchetto C, Santoro R, et al. Plasma IL8 is a biomarker for TAK1 activation and predicts resistance to nanoliposomal irinotecan in patients with gemcitabine-refractory pancreatic cancer. *Clin Cancer Res*. 2020;26:4661–4669. doi:10.1158/1078-0432.Ccr-20-0395

31. Sanmamed MF, Carranza-Rua O, Alfaro C, et al. Serum interleukin-8 reflects tumor burden and treatment response across malignancies of multiple tissue origins. *Clin Cancer Res*. 2014;20:5697–5707. doi:10.1158/1078-0432.Ccr-13-3203
32. Sanmamed MF, Perez-Gracia JL, Schalper KA, et al. Changes in serum interleukin-8 (IL-8) levels reflect and predict response to anti-PD-1 treatment in melanoma and non-small-cell lung cancer patients. *Ann Oncol*. 2017;28:1988–1995. doi:10.1093/annonc/mdx190
33. Bonavia R, Inda MM, Vandenberg S, et al. EGFRvIII promotes glioma angiogenesis and growth through the NF-κB, interleukin-8 pathway. *Oncogene*. 2012;31:4054–4066. doi:10.1038/onc.2011.563
34. Imafuji H, Matsuo Y, Ueda G, et al. Ac-quisition of gemcitabine resistance enhances angiogenesis via upregulation of IL-8 production in pancreatic cancer. *Oncol Rep*. 2019;41:3508–3516. doi:10.3892/or.2019.7105
35. Paulitti A, Andreuzzi E, Bizzotto D, et al. The ablation of the matricellular protein EMILIN2 causes defective vascularization due to impaired EGFR-dependent IL-8 production affecting tumor growth. *Oncogene*. 2018;37:3399–3414. doi:10.1038/s41388-017-0107-x
36. Sparmann A, Bar-Sagi D. Ras-induced interleukin-8 expression plays a critical role in tumor growth and angiogenesis. *Cancer Cell*. 2004;6:447–458. doi:10.1016/j.ccr.2004.09.028
37. Li W, Lin S, Li W, Wang W, Li X, Xu D. IL-8 interacts with metadherin promoting proliferation and migration in gastric cancer. *Biochem Biophys Res Commun*. 2016;478:1330–1337. doi:10.1016/j.bbrc.2016.08.123
38. Urbantat RM, Blank A, Kremenetskaia I, Vajkoczy P, Acker G, Brandenburg S. The CXCL2/IL8/CXCR2 pathway is relevant for brain tumor malignancy and endothelial cell function. *Int J Mol Sci*. 2021;22:2634. doi:10.3390/ijms22052634
39. Huang D, Ding Y, Zhou M, et al. Interleukin-8 mediates resistance to antiangiogenic agent sunitinib in renal cell carcinoma. *Cancer Res*. 2010;70:1063–1071. doi:10.1158/0008-5472.Can-09-3965
40. Meng L, Zhao Y, Bu W, et al. Bone mesenchymal stem cells are recruited via CXCL8-CXCR2 and promote EMT through TGF-β signal pathways in oral squamous carcinoma. *Cell Prolif*. 2020;53:e12859. doi:10.1111/cpr.12859